Bioenergetic consequences from xenotopic expression of a tunicate AOX in mouse mitochondria: switch from RET and ROS to FET

Article (Other)

Bioenergetic consequences from xenotopic expression of a tunicate AOX in mouse mitochondria: Switch from RET and ROS to FET

Marten Szibor, Timur Gainutdinov, Erika Fernandez-Vizarra, Eric Dufour, Zemfira Gizatullina, Grazyna Debska-Vielhaber, Juliana Heidler, Ilka Wittig, Carlo Viscomi, Frank Gellerich, Anthony L. Moore

PII: S0005-2728(19)30191-4

DOI: https://doi.org/10.1016/j.bbabio.2019.148137

Reference: BBABIO 148137

To appear in: *BBA - Bioenergetics*

Received date: 28 August 2019

Revised date: 1 December 2019

Accepted date: 5 December 2019

Please cite this article as: M. Szibor, T. Gainutdinov, E. Fernandez-Vizarra, et al., Bioenergetic consequences from xenotopic expression of a tunicate AOX in mouse mitochondria: Switch from RET and ROS to FET, *BBA - Bioenergetics*(2019), https://doi.org/10.1016/j.bbabio.2019.148137

Bioenergetic consequences from xenotopic expression of a tunicate AOX in mouse mitochondria: switch from RET and ROS to FET

Marten Szibor[a,1*], Timur Gainutdinov[b,2], Erika Fernandez-Vizarra[c,2], Eric Dufour[a], Zemfira Gizatullina[b], Grazyna Debska-Vielhaber[b], Juliana Heidler[e], Ilka Wittig[e,f], Carlo Viscomi[c], Frank Gellerich[b,3], and Anthony L. Moore[g,3]

[a]Faculty of Medicine and Health Technology, Tampere University, FI-33520 Tampere, Finland; [b]Department of Neurology, Otto-von-Guericke-University, D-39120 Magdeburg, Germany; [c]MRC Mitochondrial Biology Unit, University of Cambridge, Cambridge, CB2 0XY, UK; [d]Research Institute for Problems of Ecology and Mineral Wealth Use, Tatarstan Academy of Sciences, Kazan, Russian Federation, 420087; [e]Functional Proteomics, Faculty of Medicine, Goethe University, D-60590 Frankfurt am Main, Germany; [f]German Center for Cardiovascular Research (DZHK), Partner site RheinMain, D-60590 Frankfurt am Main, Germany; [g]Biochemistry & Biomedicine, School of Life Sciences, University of Sussex, Falmer, BN19QG Brighton, UK

[*]Address correspondence to: Marten.Szibor@tuni.fi

[1]Present address: Department of Cardiothoracic Surgery, Jena University Hospital, D-07747 Jena, Germany; Marten.Szibor@med.uni-jena.de.

[2]T.G. and E.F.-V. contributed equally to this work.

[3]F.N.G. and A.L.M. share senior authorship.

Abstract

Electron transfer from all respiratory chain dehydrogenases of the electron transport chain (ETC) converges at the level of the quinone (Q) pool. The Q redox state is thus a function of electron input (reduction) and output (oxidation) and closely reflects the mitochondrial respiratory state. Disruption of electron flux at the level of the cytochrome bc_1 complex (cIII) or cytochrome *c* oxidase (cIV) shifts the Q redox poise to a more reduced state which is generally sensed as respiratory stress. To cope with respiratory stress, many species, but not insects and vertebrates, express alternative oxidase (AOX) which acts as an electron sink for reduced Q and by-passes cIII and cIV. Here, we used *Ciona intestinalis* AOX xenotopically expressed in mouse mitochondria to study how respiratory states impact the Q poise and how AOX may be used to restore respiration. Particularly interesting is our finding that electron input through succinate dehydrogenase (cII), but not NADH:ubiquinone oxidoreductase (cI), reduces the Q pool almost entirely (>90%) irrespective of the respiratory state. AOX enhances the forward electron transport (FET) from cII thereby decreasing reverse electron transport (RET) and ROS specifically when non-phosphorylating. AOX is not engaged with cI substrates, however, unless a respiratory inhibitor is added. This sheds new light on Q poise signaling, the biological role of cII which enigmatically is the only ETC complex absent from respiratory supercomplexes but yet participates in the tricarboxylic acid (TCA) cycle. Finally, we delineate potential risks and benefits arising from therapeutic AOX transfer.

Keywords: mitochondria; OXPHOS; quinone pool; ROS; xenotopic expression; alternative oxidase (AOX)

1. Introduction

Mitochondria are cellular organelles with vital functions that range from ATP production and redox homeostasis to cellular signaling. Consequently, mitochondrial dysfunction is present in a number of the most threatening human pathologies including neurodegenerative [1] and cardiovascular diseases [2,3], obesity, diabetes mellitus [4,5], malignant cell transformation [6-8] and septic organ failure [9].

A key component for mitochondrial functions is the electron transport chain (ETC) which consists of four multi-subunit protein complexes and their redox partners. *i.e.* the quinone (Q) pool and cytochrome *c*. NADH:ubiquinone oxidoreductase (cI) and succinate dehydrogenase (cII) facilitate substrate oxidation and Q pool reduction (quinone-reducing complexes) whilst cytochrome bc_1 complex (cIII), cytochrome *c* and cytochrome *c* oxidase (cIV or COX) are the quinol-oxidizing components of the ETC. Notably, substrate oxidation and transfer of reducing equivalents through the ETC is coupled to tricarboxylic acid (TCA) cycle activity *via* cII and, in addition, to the generation of a proton-electrochemical gradient by the respiratory complexes cI, cIII and cIV. The mitochondrial membrane potential ($\Delta\psi$) is the major component of the proton-electrochemical gradient which itself is indispensable for ATP generation and mitochondrial redox homeostasis. Therefore, electron transfer from all respiratory chain dehydrogenases converges at the level of the Q pool and controlled electron flux through the ETC is the basis for metabolic homeostasis. Conversely, any blockade of cIII and cIV results in the Q pool becoming highly reduced thereby disturbing metabolic homeostasis and decreasing cellular viability [10,11]. Consequently, controlling the Q reduction state affects $\Delta\psi$ and ATP production and is of vital importance and decisive for health or disease. To cope with respiratory impairment, many species, but not insects and vertebrates, express alternative oxidase (AOX), a di-iron carboxylate protein which oxidizes the Q-pool in a non-protonmotive fashion [12] thereby acting as an electron sink for reduced Q and by-passing cIII and cIV. Such a by-pass of impaired ETC complexes by xenotopic expression of AOX has been suggested to alleviate diseases, if not offer a cure [13-15].

In previous studies, the presence of AOX in models in which ETC complexes have been disrupted has proved beneficial in restoring respiratory activity and correcting metabolism in cultured mammalian cells [16-18], fruit flies [19-22] and mice [23]. Furthermore, AOX conferred resistance to cyanide toxicity [24,25] and decreased lethality from sepsis [26]. Confusingly, AOX expression, however, had detrimental consequences in a mouse model of mitochondrial myopathy [11]. We thus sought to revisit mechanisms of ETC control in an attempt to determine how AOX expression interferes with

mammalian bioenergetics. Using isolated heart mitochondria from mice xenotopically expressing *Ciona intestinalis* AOX [25], we show that respiratory activity of cII, but not cI, causes a rapid reduction of Q (Qr > 90%) of total Q (Qt). Importantly, a high Qr/Qt state is a condition favoring reverse electron transport (RET) [10], a signaling event of pathophysiologic relevance, but has only a marginal impact on forward electron transport (FET). In different species, a high Qr/Qt state has also been identified as a pre-requisite for the engagement of AOX activity [27,28].

Here, the use of AOX revealed the extent to which the interplay of the dehydrogenases and oxidases defines the direction of electron flow (*i.e.* RET or FET). Our results also raise the question as to the legitimacy of the dual function of cII acting both, as an ETC complex and a member of the TCA cycle. Finally, the results presented in this study underline the potential benefits and risks that AOX expression may have as a diagnostic tool and/or treatment option.

2. Materials and methods

2.1 Mouse model

Ciona intestinalis alternative oxidase (AOX) coding sequence was knocked into the genomic mouse *Rosa26* locus. AOX expression was controlled by a ubiquitous and strong CAG promoter [25]. Part of the animal experiments were conducted under the 1986 UK Animals (Scientific Procedures) Act and approved by Home Office licenses (PPL: 7538 and P6C97520A) and local ethical review. All mice were kept on a C57Bl6, and WT littermates were used as controls. Animals were maintained in a temperature- and humidity-controlled facility, with a 12-h light/dark cycle and free access to water and food.

2.2 Isolation of heart mitochondria

Heart mitochondria from 12-18-week-old mice were isolated as described [29]. Briefly, hearts were rapidly removed and transferred to ice-cold MMSE-A buffer (225 mM D-mannitol (Sigma-Aldrich, M4125), 20 mM MOPS (Sigma, M1254), 75 mM sucrose (Sigma, S7903), 1 mM ethylene glycol-bis(2-aminoethylether)-*N,N,N′,N′*-tetraacetic acid (EGTA, Sigma-Aldrich, E4378), 0.5 mM DL-dithiothreitol (DTT, Sigma, 43819), pH7.4). All further steps were performed on ice. Heart tissues were minced using scissors and manually pottered in a glass-on-Teflon homogenizer until homogenous in MMSE-B buffer (MMSE-A buffer plus 0.05% nagarse, Sigma, P8038). Nagarse activity was stopped by 1:30 dilution of the homogenate in MMSE-A buffer. The homogenate was centrifuged at 2,000xg for 4 min at 4 °C and the supernatant passed through cheesecloth. The flow-through was centrifuged at 12,000xg for 10 min at 4 °C and the pellet resuspended in ice-cold MMSE-C buffer (225 mM D-mannitol, 20 mM MOPS, 75 mM sucrose, 0.1 mM EGTA, 75 mM KCl, pH7.4). Mitochondrial protein content was estimated using bicinchoninic acid assay (Pierce BCA Protein Assay Kit, Thermo Scientific, 23225) with bovine serum albumin used as standard.

2.3 Blue-native (BN) gel electrophoresis

Blue-native (BN) and BN/BN gel electrophoresis, complex I in-gel activity staining and sample preparations were performed as previously described [30,31] using ~3% digitonin (Serva, 19551) and 0.02% n-dodecyl β-maltoside (GLYCON Biochemicals, D97002-C) as detergents.

2.4 Western blot analysis

Blue-native (BN)/BN gels were blotted onto polyvinylidene difluoride (PVDF) membranes as described [30] and probed with custom-made AOX anti-serum (1:10,000; 21st Century Biochemicals) [17]. Goat anti-rabbit IgG (whole molecule)-Peroxidase antibody (Sigma, A0545) served as secondary antibody. Enhanced chemiluminescence (ECL) was used and the signal detected in a ChemiDoc XRS (Bio-Rad).

2.5 Complexome profiling

A first dimensional BN electrophoresis gel was stained with Coomassie Brilliant Blue G 250 (Serva, 17524) and the appropriate lane was cut into 96 fractions. Proteins in the gel fractions were digested using trypsin (Promega, V5111) and analyzed by mass spectrometry (MS) essentially as described [32]. MS data were analyzed by MaxQuant (v1.5.2.8) [33]. Proteins were identified using a mouse reference proteome database UniProtKB released in 6/2015 supplemented with *Ciona intestinalis* AOX. Enzyme specificity was set to trypsin. Acetylation (+42.01) at N-terminus, oxidation of methionine (+15.99), deamidation of asparagine and glutamine were selected as variable modifications and carbamidomethylation (+57.02) as fixed modification on cysteines. The false discovery rate (FDR) for the identification of proteins and peptides was 1%. Intensity-based absolute quantification (IBAQ) values were recorded. Protein abundance within native lanes were normalized to maximum appearance. Slice numbers of the maximum appearance of mitochondrial complex III dimer (483 kDa), complex IV (213 kDa), complex V (538 kDa) and respiratory supercomplex containing complex I, III dimer and one copy of complex IV (1676 kDa) were used for native mass calibration. The mass spectrometry proteomics data have been deposited to the ProteomeXchange [34] Consortium *via* the PRIDE [35] partner repository with the dataset identifier PXD014016.

2.6 Respirometry and mitochondrial ROS measurements

Mitochondrial oxygen consumption was measured using high-resolution respirometry (O2k oxygraph, Oroboros Instruments, Innsbruck, Austria) at 30 °C [36] in air-saturated medium (200 nmol O_2/ml at 95 kPa). Weight-specific oxygen consumption was calculated from the time derivative of the oxygen concentration (DatLab 7 software, Oroboros Instruments, Innsbruck, Austria). Respiration of isolated heart mitochondria (0.03 mg protein per ml) was measured in MMMP-K buffer (120 mM D-mannitol, 20 mM MOPS, 5 mM KH_2PO_4, 60 mM KCl, 5 mM $MgCl_2$, pH7.4) in the presence and absence of substrates and inhibitors as described [37]. Briefly, we used complex I substrates 10 mM pyruvate (P, Pyr, Sigma, P5280), 10 mM glutamate (G, Glu, Aldrich, 49621), 2 mM malate (M, Mal, Sigma, M1000); complex II substrate 10 mM succinate (Succ, Sigma-Aldrich, S2378) in presence or absence of 1.5 µM rotenone (ROT, Sigma-Aldrich, R8875); adenosine 5′-diphosphate (ADP, Sigma, A2754) as indicated; 5 µM carboxyatractyloside (CAT, Calbiochem, 21-620), antimycin A (AA, Sigma, A8674) as indicated; azide (Az, Sigma-Aldrich, S2002) as indicated; 1 µM carbonyl cyanide 4-(trifluoromethoxy)phenylhydrazone (FCCP, Sigma, C2920); 2.5 µM oligomycin (Sigma, O4876); 100 µM n-propyl gallate (n-PG, Sigma, P3130).

Mitochondrial ROS production was measured in parallel to oxygen consumption by attaching a fluorometer module to the respirometer and using a probe specific for the detection of H_2O_2 production [38]. Briefly, 10 µM of Amplex UltraRed Reagent (Invitrogen, A36006), 1 U/ml of peroxidase from horseradish (Sigma, P8250) and 5 U/ml of superoxide dismutase (SOD, Sigma, S8409) were added to the chamber before starting the measurement. The raw fluorescence signal was calibrated to H_2O_2 concentrations of a standard H_2O_2 solution in the presence of isolated heart mitochondria.

2.7 Qr/Qt measurements

Mitochondrial respiration and the level of Q-pool reduction were simultaneously measured voltametrically in a custom-made chamber using an oxygen electrode and a glassy carbon electrode and a platinum electrode connected to an Ag/AgCl electrode for reference essentially as previously described [39].

2.8 Measuring mitochondrial membrane potential ($\Delta\psi$)

$\Delta\psi$ was monitored fluorimetrically using 2 µM of the $\Delta\psi$-sensitive probe Safranin O (Sigma-Aldrich, S2255) as described [40]. The fluorescence signal was detected as arbitrary units (a.u.) and the signal after uncoupling with 1 µM FCCP served as zero value. $\Delta\psi$ is shown as positive value reciprocal to the fluorescence signal.

2.9 Statistical analyses

Statistical analyses were performed using GraphPad Prism (GraphPad Software, version 7.0d). 2way ANOVA was used for comparisons of at least n = 3 independent experiments and a *P* value <0.05 was considered being statistically significant. All data are shown as mean. Error bars represent standard deviations (SD).

3. Results

3.1 AOX forms homo-oligomers but does not affect the assembly or stoichiometry of other ETC complexes

We first sought to determine if AOX activity requires the recognition of specific interaction partners or if its presence affects the composition or stoichiometries of the native mouse ETC complexes. We studied this using digitonin-solubilized heart mitochondria separated by blue-native (BN) polyacrylamide gel electrophoresis [41,42]. Two mutually complementary strategies were followed. First, we digested individual gel slices by trypsin and performed mass spectrometry analysis to compose a mitochondrial complexome migration profile (Fig. 1A) [32]. In parallel, we incubated BN first dimensions with the more stringent detergent n-dodecyl β-maltoside (DDM) to in-gel dissociate high-molecular weight assemblies [30] and separated DDM-treated lanes in a second dimension (BN/BN) (Fig. 1B,C). Together, both approaches failed to identify AOX interaction partners apart from the previously described homomeric high-molecular AOX assemblies (circles in Fig. 1B,C) [25]. Importantly, AOX did not cluster with any mitochondrial protein or ETC complex with similar migration pattern (Fig. 1A), and ETC complexes showed regular migration patterns, protein composition and supercomplex stoichiometries (supplementary table S1; PRIDE dataset PXD014016). Taken together, our data confirm a xenotopically expressed tunicate AOX in the mouse as a freely diffusible redox partner.

3.2 AOX maintains phosphorylating respiration with cI substrates

A freely diffusible redox partner may pose a metabolic threat if it allows an uncontrolled ETC by-pass since electron flux through the AOX is non-protonmotive [43]. Recent experiments in which trypanosomal AOX allowed maximal NADH oxidation in submitochondrial particles from bovine heart seemingly support this notion [44]. Earlier, we observed that global AOX expression exerts no deleterious effects on the general mouse physiology whilst conferring resistance to systemic cyanide application [25], which may be accounted for by the inability of AOX to effectively compete with cIII for respiratory flux [45]. We tested this assumption in isolated intact mitochondria and found that there was little to no engagement of AOX during cI activity as reflected by the respiratory control index (RCI) of 6.9 ± 1.7 (mean ± SD, n = 8) in wild-type (WT) and 4.9 ± 1.5 (n = 7) in AOX mitochondria (Fig. 2A,B) when energized with pyruvate, glutamate and malate (PGM). Such respiration was not sensitive to n-propyl gallate (n-PG), a potent AOX inhibitor. The observed decrease in AOX RCI is based on a slightly

higher rate of non-phosphorylating respiration (state 4), *i.e.* respiration upon ADP turnover or upon inhibition of the adenine nucleotide translocase (ANT) by carboxyatractyloside (CAT) (Fig. 2B). This indicates that in the absence of respiratory inhibition only approx. 7% (or 14 nmol O_2/mg/min, blue trace in Fig. 2B) of the total electron flow is diverted to AOX. Another bioenergetic parameter for estimating the efficiency of oxidative phosphorylation is the ADP/oxygen ratio, or P/O value. It refers to the number of moles of ADP phosphorylated to ATP per two electrons flowing through the ETC to oxygen. P/O values for isolated WT and AOX heart mitochondria for different substrate combinations (supplementary Fig. S1F) are largely in agreement with literature values. Note, inhibition of two proton pumps, *i.e.* cIII and cIV by the addition of cIV inhibitor azide (Az), decreases the P/O value for AOX respiration driven by cI substrates PGM to one coupling site. It should be emphasized, however, that such measurements are notoriously inaccurate as they assume state 4 respiration (the proton leak) ceases during phosphorylating conditions which is obviously not the case when AOX is engaged (supplementary Fig. S1B). Under these conditions P/O ratios *via* an oxygen electrode are unreliable as the so-called state 4 respiration is too high (~200 nmol O_2/mg/min) to distinguish any measurable change in rate upon addition of ADP.

We reasoned that the inability of AOX to be engaged as a terminal oxidase, despite seemingly optimal conditions, may be due to its high K_M for Qr [28]. Therefore, we determined Qr/Qt ratios (in %) in parallel to respiratory rates in WT and AOX heart mitochondria energized by PGM using a Q-electrode [39]. Surprisingly, Qr/Qt values remained low (~13% Qr/Qt; Fig. 2C) and did not differ despite changing respiratory states. The failure to reach a critical threshold of Qr/Qt (blue horizontal bar in Fig. 2C) [27,28] in principle impedes an AOX engagement. In contrast, under conditions of known Q-pool reduction [28] such as upon cIII (antimycin A, AA) or cIV (azide, Az) inhibition, AOX expression allows respiratory rates in excess of 200 nmol O_2/mg/min (blue traces in Fig. 2E,F; supplementary Fig. S1A,B). Moreover, inhibitor titrations in AOX-expressing mitochondria resulted in a non-linear dependency of the respiratory rate as the levels of Qr increase [28] under non-phosphorylating conditions (Fig. 2F; supplementary Fig. S1B). The fact that AA and Az evoked similar responses make unspecific toxic inhibitor effects unlikely and Qr release due to a loss of supercomplex integrity was ruled out by measuring cI activity on a BN gel (supplementary Fig. S1C). Importantly, despite being non-protonmotive [43], AOX indirectly maintained $\Delta\psi$ in PGM energized mitochondria in the presence of AA (Fig. 2D) [46]. Such a finding is substantiated by the result that subsequent addition of cI inhibitor rotenone (ROT) collapses $\Delta\psi$ (Fig. 2D). This demonstrates that AOX can act as an effective electron

sink *in vivo* allowing phosphorylating (state 3) respiration on cI substrates when electron flux through the ETC downstream of Q is blocked.

3.3 AOX facilitates succinate-dependent FET under high protonmotive force

Similar to AOX, cII is also non-protonmotive and succinate oxidation has previously been shown to rapidly increase Qr/Qt levels to approx. 90% [28]. Since succinate is a TCA substrate, it is plausible that cII and AOX together may form a futile respiratory cycle with detrimental consequences on cell viability. Our previous results suggest that an activation of such futile cycle does not happen in the AOX mouse under non-stressed conditions [25]. To understand the mechanistic basis for this paradox, we energized isolated heart mitochondria with succinate and measured respiratory rates in the presence of ROT (Fig. 3A). Our data reveal that succinate rapidly reduces the Q-pool above a critical threshold (blue horizontal bar in Fig. 3B) without generating relevant amount of mitochondrial reactive oxygen species (ROS) under any respiratory state (Fig. 3C) and that the presence of AOX does indeed enhance mitochondrial respiratory rates both under phosphorylating (presence of ADP, state 3) and non-phosphorylating (absence of ADP, state 4) conditions (Fig. 3A). Diversion of electron flux through AOX is also reflected by a decrease in RCI from 3.2 ± 0.5 (mean ± SD, n = 5) in WT to 1.3 ± 0.1 (n = 7) in AOX mitochondria (supplementary Fig. S1D,E). Interestingly, the respiratory rate has little, if any, effect on the Qr/Qt ratios (Fig. 3B). Similar to cI substrates, $\Delta\psi$ is still maintained during succinate-driven respiration (Fig. 3D), suggesting that even in the presence of AOX, a significant proportion of the electron flux is mediated *via* the proton-pumping activities of cIII and cIV (representative traces shown in Fig. 3E,F). P/O values were also calculated for succinate-dependent respiration in WT heart mitochondria (supplementary Fig. S1F). As indicated previously, AOX activity is a complicating factor during succinate-dependent respiration (both in the presence and absence of ADP, respectively). This prevents any accurate calculation of P/O values with AOX respiring mitochondria. In support of such a notion, it is apparent from the original respiratory traces (supplementary Fig. S1D,E) that the P/O ratio of isolated AOX heart mitochondria must be significantly lower than in WT even if an accurate number cannot be reliably determined because of the high basal respiratory rate.

3.4 AOX prevents RET under non-phosphorylating conditions

Succinate accumulation along with high $\Delta\psi$ and Qr/Qt has been described as mechanism for RET [10] in ischemia-reperfusion injury and inflammatory diseases [26,47,48]. For the latter, AOX was demonstrated to have beneficial effects [26]. The bioenergetic rationale for such beneficial effects was believed to depend upon the ability of AOX to maintain the Q-pool in a more oxidized state in comparison to WT mitochondria thereby reducing RET-mediated ROS production [10,25]. We sought to test if this was the case by determining how AOX exerts its effects on mitochondrial respiration on succinate in the absence of ROT and thus in the presence of a fully functional cI. Again, isolated heart mitochondria expressing AOX were used and we discovered enhanced succinate-driven respiration under non-phosphorylating conditions (Fig. 4A; supplementary Fig. S1G). Although the addition of small amounts of ADP increased respiration in WT mitochondria, the presence of AOX had no additive effect (Fig. 4A; supplementary Fig. S1G). The addition of saturating amounts of ADP failed to induce sustained phosphorylating respiration (Fig. 4A; supplementary Fig. S1G) both in WT and AOX heart mitochondria. This was previously attributed to a loss of $\Delta\psi$ and the generation of the potent cII inhibitor oxaloacetate [49]. As demonstrated here (Fig. 4D), such a notion is not supported by $\Delta\psi$ measurements (original traces shown in Fig. 4E,F). Although addition of ADP severely diminished the magnitude of $\Delta\psi$, the fact that it is restored upon ANT inhibition by CAT (Fig. 4D), suggests that the observed depolarization is due to ATP/ADP exchange and not due to a proposed inhibition of cII activity [49]. In support of this notion, respiratory uncoupling by carbonyl cyanide 4-(trifluoromethoxy)phenylhydrazone (FCCP) following CAT fully depolarizes $\Delta\psi$ (Fig. 4D-F). Furthermore, measurements of the steady-state redox poise of the Q-pool in the absence of ROT showed that the pool is highly reduced irrespective of the respiratory state and presence or absence of ADP and/or AOX (Fig. 4B). Although the subsequent addition of PGM and/or ROT in the presence of succinate dramatically increased respiratory rates (Fig. 4A; supplementary Fig. S1G) addition of ROT caused negligible Q oxidation (Fig. 4B). Of particular importance is the observation that the presence of AOX, in the absence of ROT, substantially reduces ROS production in comparison to WT mitochondria (Fig. 4C; supplementary Fig. S1H) both in the presence of succinate alone or under non-phosphorylating conditions. Such results indicate that under pathologic conditions, AOX can shift the electron flux through the ETC from RET (and ROS) towards FET.

4. Discussion

In the present study, we confirm that AOX from the tunicate *Ciona intestinalis* functions as a freely diffusible mitochondrial oxidase potentially without mobility restrictions when xenotopically expressed in the mouse (Fig. 1A). This may seem surprising considering the formation of high-molecular weight assemblies which have previously been described as mainly homo-oligomers of dimers [25]. Indeed, it is unclear thus far, which assembly stoichiometry may constitute the most active AOX form in the mouse *in vivo*. Interestingly, the expression of AOX as dimer was first described for plants and its reduction state was related to its catalytic activity [50]. Later it was proposed that AOX dimerization is common to all AOXs and that such assemblies may be of mechanistic or structural importance [12,51,52]. Respiratory stress may result in the buildup of reducing equivalents within the mitochondrial matrix thereby facilitating the reduction of regulatory residues, e.g. cysteines forming disulfide bonds [50]. It is unlikely, however, that this mechanism controls AOX activity in its host *Ciona intestinalis* since this tunicate AOX does not contain the conserved cysteine residues necessary for activation as is the case in plants. How homo-oligomerization of xenotopically expressed tunicate AOX in the mouse affects its catalytic engagement cannot be concluded with absolute certainty to date, however, it is obvious from this and previous studies that a xenotopically expressed tunicate AOX is highly active. Furthermore, apart from the formation of homo-oligomers, AOX association with supercomplexes has never been demonstrated although it is conceivable, albeit unlikely, that the inclusion of digitonin may have removed AOX from high-molecular structures. Altogether, this supports the notion that xenotopically expressed AOX acts as a freely diffusible redox partner. Indeed, when trypansomal AOX was added to submitochondrial particles (SMPs) in the presence of cyanide, respiratory activity was restored [44] from which it was concluded that Q channeling in mitochondrial supercomplexes does not exist. We found, however, that in isolated mouse heart mitochondria respiring on cI substrates in the absence of respiratory inhibitors AOX only marginally affected the RCI suggesting that under these conditions AOX was barely engaged (Fig. 2B). Such a lack of engagement was substantiated by the discovery that in the absence of respiratory inhibitors the Q-pool is insufficiently reduced by cI to maintain AOX activity (Fig. 2C). Addition of respiratory inhibitors, however, engages AOX both under phosphorylating (state 3) [25] and non-phosphorylating (state 4) conditions (Fig. 2E,F; supplementary Fig. S1A,B) whilst maintaining $\Delta\psi$ (Fig. 2D). Of course, the measured global Qr/Qt ratio cannot exclude different local Qr/Qt conditions, for instance in a putative compartment within respirasomes between cI and cIII [53]. The fact that AOX and Q are freely diffusible, yet cI substrates do not support high AOX respiration,

however, indicate that such high Qr/Qt ratios are not achieved or immediately decreased through oxidation by cIII. Titration of cI activity with AA or Az, however, resulted in an exponential increase in the presence of AOX (Fig. 2F; supplementary Fig. S1B) suggesting that the pool is accessible to AOX under all Qr/Qt ratios. This is of importance for the biological function of AOX, e.g. during stress response. It has recently been shown in its natural host, *Ciona intestinalis*, that AOX transcript levels are upregulated upon exposure to hypoxia and by sulfide, a potent cIV inhibitor, whilst being unresponsive to other environmental stressors such as physiologically stressful temperature or heavy-metal exposure [54]. Here, due to the genetic design, AOX transcript level cannot directly correlate with its catalytic function. In fact, our results explain the lack of a detrimental phenotype when AOX protein is ubiquitously expressed in the mouse despite its ability to resist cyanide intoxication [24,25].

Although, AOX confers resistance to cyanide, the failure to rescue a COX15 knock-out in mouse skeletal muscle at first appeared somewhat mysterious. However, it may be explained by the fact that under disease and respiratory stress conditions, the metabolic situation is different. One major difference between the acute application of cyanide and the permanent ablation of COX15 is that the long-term disruption of signaling cascades required for mitochondrial biogenesis and muscle repair may outweigh potential benefits such as a decreased ROS load. In contrast, succinate accumulation and RET induction has been described for the post-ischemic heart and sepsis [26,47] and for the latter AOX expression showed beneficial effects [26]. Of note, all aforementioned examples concentrate on a putative effect of AOX on pathophysiologic conditions while seemingly ignoring physiological signals originating from the respiratory chain. In fact, some stress responses related to mitochondrial dysfunction viewed as detrimental thus far, such as ROS emitted from COX15 deficient mitochondria [11], are now recognized as essential for adaptive remodeling, mitochondrial biosynthesis and survival. In other words, mitochondrial ROS may be of vital importance for adaptation and thus having physiological relevance. This is specifically true for oxygen sensing in the pulmonary vasculature [55] and glomus cells of the carotid body [56]. In both cases, signals from the respiratory chain are required, and an increase of the Qr/Qt ratio can safely be assumed or has been demonstrated. It is tempting to speculate how AOX would interfere with oxygen sensing in the two cell types considering their specific physiological function and what role succinate may play under such conditions. In an attempt to replicate the above-described metabolic situations, we tested AOX heart mitochondria in the presence of succinate plus ROT (to prevent RET) and observed high respiratory activity even in the absence of ADP which, importantly, was associated with a dramatic decrease in the RCI (also seen as high state 4 respiration in

Fig. 3A) suggesting that AOX was engaged. Since cII is generally not present in supercomplex assemblies, the observed respiration is likely based on random collision of the three independent freely diffusible redox partners, *i.e.* cII, the Q pool and AOX. Qr/Qt measurements revealed that in the presence of cII substrate succinate, irrespective of the presence or absence of ROT, another criterion for AOX engagement is fulfilled, namely the presence of high Qr/Qt ratios (Fig. 3B; 4B). In plants, engagement of the alternative respiratory pathway occurs only when Qr/Qt ratios reach critical thresholds of 35-40% (blue horizontal bars in Fig. 2C; 3B; 4B) [27,28]. Previously, *Ciona intestinalis* AOX expressed in mouse skeletal muscle has revealed strikingly similar Qr/Qt values for catalytic engagement [11]. Surprisingly, we found AOX to be regularly engaged during cII respiration under non-phosphorylating (state 4) but not phosphorylating (state 3) conditions although never achieving maximal respiratory rates (Fig. 3A; 4A) suggesting there is some restriction of electron flow. Importantly, our findings demonstrate that any observed restriction of electron flow is not necessarily due to a lack of Q-pool reduction as Qr levels remain high (Fig. 3B; 4B). It may be due to a loss of $\Delta\psi$ [49] although addition of ADP depolarizes $\Delta\psi$ which is CAT-insensitive and thus not due to phosphorylation (Fig. 3D-F; 4D-F). Obviously, some electron flux continues to be mediated by cIII as $\Delta\psi$ is still maintained even with AOX. The finding that electron flux through AOX, in the absence of ROT, is very low may suggest that the regulated element may be cII itself, possibly as a result of oxaloacetate accumulation [49]. If AOX is engaged, however, it supports respiration and abolishes mitochondrial ROS production by RET in a similar manner to ADP addition (Fig. 4A,C). Altogether, our data support the notion that *in vivo* succinate is unlikely to be a major respiratory substrate since a non-phosphorylating respiratory shunt (cII-Q-AOX), would inevitably lead to a severe, non-viable, phenotype which is obviously not the case [25].

Interestingly, the Qr/Qt ratios appear unaffected by any changes of the respiratory state (Fig. 2C; 3B; 4B). Thus, although Qr is fully reduced and potentially accessible to AOX, respiration is low under phosphorylating (state 3) yet high under non-phosphorylating (state 4) conditions (Fig. 4A; supplementary Fig. S1G). A high electron flux through cII in the presence of oxaloacetate is not likely and contrary to expectations a decrease in the Qr/Qt ratio was not observed. More importantly, when cI substrates were added to the mitochondria we observed an increase in phosphorylating, oligomycin-sensitive, respiration and a decrease in ROS production (supplementary Fig. S1G,H). Such stimulation, however, is not solely dependent on an increase in $\Delta\psi$ or electron flow through cI since ROT addition showed the same result (Fig. 4A,C). This finding raises questions regarding the true function of cII *in*

vivo in health and disease. We propose that under disease conditions, cII-induced RET may be a pivotal signal for adaptation. Under all other conditions, regular succinate levels in the presence of ADP, RET and FET seem to be restricted by a number of possible factors, including cI presence and, may be, its catalytic activity. The fact that a minimum of 84% of cI is complexed in respiratory supercomplexes [42] suggests that some sort of Q flux control or Q compartmentalization may be potentially a reason for the development of supercomplexes.

In conclusion, xenotopically expressed tunicate AOX is a freely diffusible redox partner in mouse mitochondria which is catalytically active when the Q pool is highly reduced (summarized in Fig. 5). However, respiratory engagement is favored under non-phosphorylating (state 4) conditions generally described as respiratory stress. AOX thus is an invaluable tool to investigate respiratory control mechanisms and may become a treatment option for mitochondriopathies based on respiratory disruption.

Acknowledgements: The authors thank Howard T. Jacobs, Pierre Rustin and Massimo Zeviani for valuable discussions and support, and Jana Meisterknecht for excellent technical assistance. This work was supported by: the ERC Advanced Grants 232738 and 322424 to Howard T. Jacobs and Massimo Zeviani, respectively, and Academy of Finland grants 272376 and 256615 to Howard T. Jacobs; the Deutsche Forschungsgemeinschaft (SFB 815/Z1) and the BMBF mitoNET-German Network for Mitochondrial Disorders (01GM1906D) to I.W.; BBSRC (BB/N010051/1) to A.L.M.; and a core grant of the MRC (MC_UU_00015/5) to the Mitochondrial Biology Unit.

Author contributions: M.S. designed and supervised research; M.S., Z.G., E.F.-V., E.D. G.D.-V., T.G., J.H., I.W., C.V., F.N.G., and A.L.M. performed research; M.S., E.F.-V., I.W., E.D., C.V., F.N.G., and A.L.M. compiled and analyzed data; M.S., C.V., F.N.G., and A.L.M. drafted the manuscript with support from all authors.

Conflict of interest statement: M.S. declares himself as a shareholder in a start-up company to develop therapeutics based on alternative oxidase. All other authors declare no competing interests.

References

[1] S. DiMauro, E.A. Schon, Mitochondrial disorders in the nervous system, Annu. Rev. Neurosci. 31 (2008) 91–123. doi:10.1146/annurev.neuro.30.051606.094302.

[2] E. Bertero, C. Maack, Metabolic remodelling in heart failure, Nat Rev Cardiol. 15 (2018) 457–470. doi:10.1038/s41569-018-0044-6.

[3] E. Murphy, H. Ardehali, R.S. Balaban, F. DiLisa, G.W. Dorn, R.N. Kitsis, et al., Mitochondrial Function, Biology, and Role in Disease: A Scientific Statement From the American Heart Association, Circ Res. 118 (2016) 1960–1991. doi:10.1161/RES.0000000000000104.

[4] A. Gonzalez-Franquesa, M.-E. Patti, Insulin Resistance and Mitochondrial Dysfunction, Adv. Exp. Med. Biol. 982 (2017) 465–520. doi:10.1007/978-3-319-55330-6_25.

[5] M. Liesa, O.S. Shirihai, Mitochondrial dynamics in the regulation of nutrient utilization and energy expenditure, Cell Metabolism. 17 (2013) 491–506. doi:10.1016/j.cmet.2013.03.002.

[6] S.S. Sabharwal, P.T. Schumacker, Mitochondrial ROS in cancer: initiators, amplifiers or an Achilles' heel? Nat Rev Cancer. 14 (2014) 709–721. doi:10.1038/nrc3803.

[7] P. Pinton, G. Kroemer, Cancer therapy: Altering mitochondrial properties, Nat Chem Biol. 10 (2014) 89–90. doi:10.1038/nchembio.1440.

[8] W.H. Koppenol, P.L. Bounds, C.V. Dang, Otto Warburg's contributions to current concepts of cancer metabolism, Nat Rev Cancer. 11 (2011) 325–337. doi:10.1038/nrc3038.

[9] M. Singer, The role of mitochondrial dysfunction in sepsis-induced multi-organ failure, Virulence. 5 (2014) 66–72. doi:10.4161/viru.26907.

[10] E.L. Robb, A.R. Hall, T.A. Prime, S. Eaton, M. Szibor, C. Viscomi, et al., Control of mitochondrial superoxide production by reverse electron transport at complex I, J Biol Chem. 293 (2018) 9869–9879. doi:10.1074/jbc.RA118.003647.

[11] S.A. Dogan, R. Cerutti, C. Benincá, G. Brea-Calvo, H.T. Jacobs, M. Zeviani, et al., Perturbed Redox Signaling Exacerbates a Mitochondrial Myopathy, Cell Metabolism. 28 (2018) 764–775.e5. doi:10.1016/j.cmet.2018.07.012.

[12] A.L. Moore, T. Shiba, L. Young, S. Harada, K. Kita, K. Ito, Unraveling the heater: new insights into the structure of the alternative oxidase, Annu Rev Plant Biol. 64 (2013) 637–663. doi:10.1146/annurev-arplant-042811-105432.

[13] S. DiMauro, M. Hirano, E.A. Schon, Approaches to the treatment of mitochondrial diseases, Muscle Nerve. 34 (2006) 265–283. doi:10.1002/mus.20598.

[14] R. El-Khoury, K.K. Kemppainen, E. Dufour, M. Szibor, H.T. Jacobs, P. Rustin, Engineering the alternative oxidase gene to better understand and counteract mitochondrial defects: state of the art and perspectives, Br J Pharmacol. 171 (2014) 2243–2249. doi:10.1111/bph.12570.

[15] P. Rustin, H.T. Jacobs, Respiratory chain alternative enzymes as tools to better understand and counteract respiratory chain deficiencies in human cells and animals, Physiol Plant. 137 (2009) 362–370. doi:10.1111/j.1399-3054.2009.01249.x.

[16] G.A.J. Hakkaart, E.P. Dassa, H.T. Jacobs, P. Rustin, Allotopic expression of a mitochondrial alternative oxidase confers cyanide resistance to human cell respiration, EMBO Rep. 7 (2006) 341–345. doi:10.1038/sj.embor.7400601.

[17] E.P. Dassa, E. Dufour, S. Goncalves, V. Paupe, G.A.J. Hakkaart, H.T. Jacobs, et al., Expression of the alternative oxidase complements cytochrome c oxidase deficiency in human cells, EMBO Mol Med. 1 (2009) 30–36. doi:10.1002/emmm.200900001.

[18] E.P. Dassa, E. Dufour, S. Goncalves, H.T. Jacobs, P. Rustin, The alternative oxidase, a tool for compensating cytochrome c oxidase deficiency in human cells, Physiol Plant. 137 (2009) 427–434. doi:10.1111/j.1399-3054.2009.01248.x.

[19] D.J.M. Fernández-Ayala, A. Sanz, S. Vartiainen, K.K. Kemppainen, M. Babusiak, E. Mustalahti, et al., Expression of the Ciona intestinalis alternative oxidase (AOX) in Drosophila complements defects in mitochondrial oxidative phosphorylation, Cell Metabolism. 9 (2009) 449–460. doi:10.1016/j.cmet.2009.03.004.

[20] D.M. Humphrey, R.B. Parsons, Z.N. Ludlow, T. Riemensperger, G. Esposito, P. Verstreken, et al., Alternative oxidase rescues mitochondria-mediated dopaminergic cell loss in Drosophila, Human Molecular Genetics. 21 (2012) 2698–2712. doi:10.1093/hmg/dds096.

[21] K.K. Kemppainen, J. Rinne, A. Sriram, M. Lakanmaa, A. Zeb, T. Tuomela, et al., Expression of alternative oxidase in Drosophila ameliorates diverse phenotypes due to cytochrome oxidase deficiency, Human Molecular Genetics. 23 (2014) 2078–2093. doi:10.1093/hmg/ddt601.

[22] S. Vartiainen, S. Chen, J. George, T. Tuomela, K.R. Luoto, K.M.C. O'Dell, et al., Phenotypic rescue of a Drosophila model of mitochondrial ANT1 disease, Dis Model Mech. 7 (2014) 635–648. doi:10.1242/dmm.016527.

[23] R. El-Khoury, E. Kaulio, K.A. Lassila, D.C. Crowther, H.T. Jacobs, P. Rustin, Expression of the alternative oxidase mitigates beta-amyloid production and toxicity in model systems, Free Radic Biol Med. 96 (2016) 57–66. doi:10.1016/j.freeradbiomed.2016.04.006.

[24] R. El-Khoury, E. Dufour, M. Rak, N. Ramanantsoa, N. Grandchamp, Z. Csaba, et al., Alternative oxidase expression in the mouse enables bypassing cytochrome c oxidase blockade and limits mitochondrial ROS overproduction, PLoS Genet. 9 (2013) e1003182. doi:10.1371/journal.pgen.1003182.

[25] M. Szibor, P.K. Dhandapani, E. Dufour, K.M. Holmström, Y. Zhuang, I. Salwig, et al., Broad AOX expression in a genetically tractable mouse model does not disturb normal physiology, Dis Model Mech. 10 (2017) 163–171. doi:10.1242/dmm.027839.

[26] E.L. Mills, B. Kelly, A. Logan, A.S.H. Costa, M. Varma, C.E. Bryant, et al., Succinate Dehydrogenase Supports Metabolic Repurposing of Mitochondria to Drive Inflammatory Macrophages, Cell. 167 (2016) 457–470.e13. doi:10.1016/j.cell.2016.08.064.

[27] I.B. Dry, A.L. Moore, D.A. Day, J.T. Wiskich, Regulation of alternative pathway activity in plant mitochondria: nonlinear relationship between electron flux and the redox poise of the quinone pool, Archives of Biochemistry and Biophysics. 273 (1989) 148–157.

[28] C. Affourtit, K. Krab, A.L. Moore, Control of plant mitochondrial respiration, Biochim Biophys Acta. 1504 (2001) 58–69.

[29] M. Fontana-Ayoub, G. Krumschnabel, Laboratory protocol: isolation of mouse heart mitochondria, Mitochondrial Physiology Network. 20.06(01) (2015) 1–2.

[30] I. Wittig, H.-P. Braun, H. Schägger, Blue native PAGE, Nat Protoc. 1 (2006) 418–428. doi:10.1038/nprot.2006.62.

[31] I. Wittig, M. Karas, H. Schägger, High resolution clear native electrophoresis for in-gel functional assays and fluorescence studies of membrane protein complexes, Mol Cell Proteomics. 6 (2007) 1215–1225. doi:10.1074/mcp.M700076-MCP200.

[32] H. Heide, L. Bleier, M. Steger, J. Ackermann, S. Dröse, B. Schwamb, et al., Complexome profiling identifies TMEM126B as a component of the mitochondrial complex I assembly complex, Cell Metabolism. 16 (2012) 538–549. doi:10.1016/j.cmet.2012.08.009.

[33] J. Cox, M. Mann, MaxQuant enables high peptide identification rates, individualized p.p.b.-range mass accuracies and proteome-wide protein quantification, Nat Biotechnol. 26 (2008) 1367–1372. doi:10.1038/nbt.1511.

[34] E.W. Deutsch, A. Csordás, Z. Sun, A. Jarnuczak, Y. Perez-Riverol, T. Ternent, et al., The ProteomeXchange consortium in 2017: supporting the cultural change in proteomics public data deposition, Nucleic Acids Res. 45 (2017) D1100–D1106. doi:10.1093/nar/gkw936.

[35] Y. Perez-Riverol, A. Csordás, J. Bai, M. Bernal-Llinares, S. Hewapathirana, D.J. Kundu, et al., The PRIDE database and related tools and resources in 2019: improving support for quantification data, Nucleic Acids Res. 47 (2019) D442–D450. doi:10.1093/nar/gky1106.

[36] E. Gnaiger, Bioenergetics at low oxygen: dependence of respiration and phosphorylation on oxygen and adenosine diphosphate supply, Respir Physiol. 128 (2001) 277–297.

[37] Z.Z. Gizatullina, T.M. Gaynutdinov, H. Svoboda, D. Jerzembek, A. Knabe, S. Vielhaber, et al., Effects of cyclosporine A and its immunosuppressive or non-immunosuppressive derivatives [D-Ser]8-CsA and Cs9 on mitochondria from different brain regions, Mitochondrion. 11 (2011) 421–429. doi:10.1016/j.mito.2010.12.012.

[38] G. Krumschnabel, M. Fontana-Ayoub, Z. Sumbalova, J. Heidler, K. Gauper, M. Fasching, et al., Simultaneous high-resolution measurement of mitochondrial respiration and hydrogen peroxide production, Methods Mol Biol. 1264 (2015) 245–261. doi:10.1007/978-1-4939-2257-4_22.

[39] A.L. Moore, I.B. Dry, J.T. Wiskich, Measurement of the redox state of the ubiquinone pool in plant mitochondria, FEBS Letters. 235 (1988) 76–80. doi:10.1016/0014-5793(88)81237-7.

[40] F.N. Gellerich, Z. Gizatullina, S. Trumbekaite, B. Korzeniewski, T. Gaynutdinov, E. Seppet, et al., Cytosolic Ca2+ regulates the energization of isolated brain mitochondria by formation of pyruvate through the malate-aspartate shuttle, Biochem J. 443 (2012) 747–755. doi:10.1042/BJ20110765.

[41] I. Wittig, R. Carrozzo, F.M. Santorelli, H. Schägger, Supercomplexes and subcomplexes of mitochondrial oxidative phosphorylation, Biochim Biophys Acta. 1757 (2006) 1066–1072. doi:10.1016/j.bbabio.2006.05.006.

[42] H. Schägger, K. Pfeiffer, The ratio of oxidative phosphorylation complexes I-V in bovine heart mitochondria and the composition of respiratory chain supercomplexes, J Biol Chem. 276 (2001) 37861–37867. doi:10.1074/jbc.M106474200.

[43] A.L. Moore, W.D. Bonner, P.R. Rich, The determination of the proton-motive force during cyanide-insensitive respiration in plant mitochondria, Archives of Biochemistry and Biophysics. 186 (1978) 298–306.

[44] J.G. Fedor, J. Hirst, Mitochondrial Supercomplexes Do Not Enhance Catalysis by Quinone Channeling, Cell Metabolism. 28 (2018) 525–531.e4. doi:10.1016/j.cmet.2018.05.024.

[45] Y. Kido, K. Sakamoto, K. Nakamura, M. Harada, T. Suzuki, Y. Yabu, et al., Purification and kinetic characterization of recombinant alternative oxidase from Trypanosoma brucei brucei, Biochim Biophys Acta. 1797 (2010) 443–450. doi:10.1016/j.bbabio.2009.12.021.

[46] A.L. Moore, W.D. Bonner, Measurements of membrane potentials in plant mitochondria with the safranine method, Plant Physiology. 70 (1982) 1271–1276.

[47] E.T. Chouchani, V.R. Pell, E. Gaude, D. Aksentijević, S.Y. Sundier, E.L. Robb, et al., Ischaemic accumulation of succinate controls reperfusion injury through mitochondrial ROS, Nature. 515 (2014) 431–435. doi:10.1038/nature13909.

[48] F. Scialò, A. Sriram, D. Fernández-Ayala, N. Gubina, M. Lõhmus, G. Nelson, et al., Mitochondrial ROS Produced via Reverse Electron Transport Extend Animal Lifespan, Cell Metabolism. 23 (2016) 725–734. doi:10.1016/j.cmet.2016.03.009.

[49] F. Bai, B.D. Fink, L. Yu, W.I. Sivitz, Voltage-Dependent Regulation of Complex II Energized Mitochondrial Oxygen Flux, PLoS ONE. 11 (2016) e0154982. doi:10.1371/journal.pone.0154982.

[50] A.L. Umbach, J.N. Siedow, Covalent and Noncovalent Dimers of the Cyanide-Resistant Alternative Oxidase Protein in Higher Plant Mitochondria and Their Relationship to Enzyme Activity, Plant Physiology. 103 (1993) 845–854. doi:10.1104/pp.103.3.845.

[51] T. Shiba, Y. Kido, K. Sakamoto, D.K. Inaoka, C. Tsuge, R. Tatsumi, et al., Structure of the trypanosome cyanide-insensitive alternative oxidase, Proc Natl Acad Sci USA. 110 (2013) 4580–4585. doi:10.1073/pnas.1218386110.

[52] B. May, L. Young, A.L. Moore, Structural insights into the alternative oxidases: are all oxidases made equal? Biochem Soc Trans. 45 (2017) 731–740. doi:10.1042/BST20160178.

[53] G. Benard, B. Faustin, A. Galinier, C. Rocher, N. Bellance, K. Smolkova, et al., Functional dynamic compartmentalization of respiratory chain intermediate substrates: implications for the control of energy production and mitochondrial diseases, International Journal of Biochemistry and Cell Biology. 40 (2008) 1543–1554. doi:10.1016/j.biocel.2007.11.023.

[54] S. Saari, G.S. Garcia, K. Bremer, M.M. Chioda, A. Andjelković, P.V. Debes, et al., Alternative respiratory chain enzymes: Therapeutic potential and possible pitfalls, Biochim Biophys Acta Mol Basis Dis. 1865 (2019) 854–866. doi:10.1016/j.bbadis.2018.10.012.

[55] N. Sommer, M. Hüttemann, O. Pak, S. Scheibe, F. Knoepp, C. Sinkler, et al., Mitochondrial Complex IV Subunit 4 Isoform 2 Is Essential for Acute Pulmonary Oxygen Sensing, Circ Res. 121 (2017) 424–438. doi:10.1161/CIRCRESAHA.116.310482.

[56] I. Arias-Mayenco, P. González-Rodríguez, H. Torres-Torrelo, L. Gao, M.C. Fernández-Agüera, V. Bonilla-Henao, et al., Acute O2 Sensing: Role of Coenzyme QH2/Q Ratio and Mitochondrial ROS Compartmentalization, Cell Metabolism. 28 (2018) 145–158.e4. doi:10.1016/j.cmet.2018.05.009.

Figure legends

Fig. 1. AOX acts as a freely diffusible Qr redox partner. (**A**) Digitonin-solubilized AOX heart mitochondria separated by 1D blue-native (BN) polyacrylamide gel electrophoresis, analyzed by mass spectrometry. Heat maps of selected protein subunits representing individual respiratory complexes with red color representing a high and black color representing a low expression. cI, Ndufs7; cIII, Uqcrc1; cIV, Cox4i1; cV, Atp5a1; cII, Sdha. Line-chart to illustrate the migration pattern of classical respiratory complexes and AOX assemblies. Note, estimated molecular masses support the notion that AOX expressed in the mouse assembles into homo-oligomers mainly consisting of multimers of dimers. (**B**) Coomassie stain of digitonin-solubilized AOX heart mitochondria separated by tandem BN/BN using n-dodecyl β-maltoside (DDM) treatment before second dimensional run. (**C**) AOX protein detected by western blot analysis. Of note, the regular pattern of AOX assemblies marked by circles again indicates that AOX does not form erratic aggregates but rather assembles into multimers of different stoichiometries. Circles from the western blot analysis have been superposed onto the Coomassie stained gel to visualize the AOX multimer migration pattern in comparison to other mitochondrial complexes.

Fig. 2. AOX is engaged on cI substrates only in the presence of respiratory inhibitors. Representative respirometry traces of isolated WT (**A**) and AOX (**B**) heart mitochondria respiring on cI substrates pyruvate, glutamate and malate (PGM) with adenosine diphosphate (ADP in µM) and carboxyatractyloside (CAT) additions as indicated. Respiratory control indices (RCI) shown as mean ± SD, WT n = 8, AOX n = 7. (**C**) Qr/Qt ratios (%) shown as mean ± SD, n = 3. Blue horizontal bar represents putative threshold for AOX engagement. (**D**) Mitochondrial membrane potential ($\Delta\psi$) shown as arbitrary units (a.u.) as mean ± SD, n = 3. AA, antimycin A. Grey area indicates significant difference between WT and AOX ($P < 0.05$) analyzed by 2way ANOVA with post-hoc Sidak's multiple comparisons test. Representative respiratory rate traces of isolated WT and AOX heart mitochondria in non-phosphorylating (absence of ADP, state 4) (**E**) and phosphorylating (presence of ADP, state 3) (**F**) conditions with PGM as substrates. ADP (in µM) and AA (in µM) additions as indicated.

Fig. 3. AOX engages on cII substrate succinate when cI is inhibited. (**A**) Respiratory rates of isolated heart mitochondria shown as mean ± SD, n = 3. ROT, rotenone; ADP in µM. Grey areas indicate significant difference between WT and AOX ($P < 0.05$) analyzed by 2way ANOVA with post-hoc Sidak's

multiple comparisons test. (**B**) Qr/Qt ratios (%) shown as mean ± SD, n = 3. Blue horizontal bar represents putative threshold for AOX engagement. (**C**) Hydrogen peroxide production shown as mean ± SD, n = 3. (**D**) Mitochondrial membrane potential ($\Delta\psi$) using safranin O shown as mean ± SD, n = 3. (**E**) Representative trace showing $\Delta\psi$ under conditions as indicated in WT mitochondria. (**F**) Representative trace showing $\Delta\psi$ under conditions as indicated in AOX mitochondria.

Fig. 4. AOX engages on cII substrate succinate only under non-phosphorylating conditions. (**A**) Respiratory rates of isolated heart mitochondria shown as mean ± SD, n = 3. ADP in µM; ROT, rotenone. Grey areas indicate significant difference between WT and AOX ($P < 0.05$) analyzed by 2way ANOVA with post-hoc Sidak's multiple comparisons test. (**B**) Qr/Qt ratios (%) shown as mean ± SD, n = 3. Blue horizontal bar represents putative threshold for AOX engagement. (**C**) Hydrogen peroxide production shown as mean ± SD, n = 3. Grey areas indicate significant difference between WT and AOX ($P < 0.05$) analyzed by 2way ANOVA with post-hoc Sidak's multiple comparisons test. Note the inverse relation of hydrogen peroxide production and respiratory rate. (**D**) Mitochondrial membrane potential ($\Delta\psi$) using safranin O shown as mean ± SD, n = 3. Note the lack of membrane potential restoration in state 3. (**E**) Representative trace showing $\Delta\psi$ under conditions as indicated in WT mitochondria. (**F**) Representative trace showing $\Delta\psi$ under conditions as indicated in AOX mitochondria.

Fig. 5. Graphical overview on AOX engagement. (**A**) cI substrates do not allow AOX respiration unless cIII and/or cIV are inhibited. AA, antimycin A. (**B**) cII substrate succinate readily engages AOX when cI is inhibited (ROT, rotenone) or in the absence of ADP. Note, ROT acts upstream of Q thus being indicative for a cI control mechanism on AOX engagement independent from the Qr/Qt ratio.

Supplementary material

Mass spectrometry proteomics data.

Deposited to the ProteomeXchange Consortium *via* the PRIDE [35] partner repository (dataset identifier - PXD014016).

Supplementary table S1. Selected complexome profiles from AOX transgenic mouse heart mitochondria (relates to Fig. 1A).

Supplementary Fig. S1. AOX engagement in mitochondrial respiration (relates to Fig. 2E,F; Fig. 3A; 4A,C). Representative respiratory rate traces of isolated WT and AOX heart mitochondria in phosphorylating (presence of ADP, state 3) (**A**) and non-phosphorylating (absence of ADP, state 4) (**B**) conditions with PGM as substrates. ADP (in µM) and azide (Az, in mM) additions as indicated. (**C**) cI in-gel staining of isolated WT and AOX heart mitochondria treated with Antimycin A (AA) as indicated separated on a blue-native (BN) gel. BHM, bovine heart mitochondria, used as control. Assignment of complexes: S_0, supercomplexes containing complex I and III with the stoichiometry of I_1III_2; S_{1-3}, supercomplexes containing complex I, III and IV with the stoichiometry of $I_1III_2IV_{1-3}$; S_{XL}, large supercomplexes; III_2, dimer of complex III or cytochrome c reductase; IV, complex IV or cytochrome c oxidase; V, complex V or ATP synthase. Representative respiratory rate traces of isolated WT (**D**) and AOX (**E**) heart mitochondria in state 3 or state 4 as indicated with succinate as substrate. (**F**) Table of P/O values for isolated WT and AOX heart mitochondria respiring on substrates as indicated. Data are shown as mean ± SD of n = 3 measurements. $P < 0.05$ tested by 1way ANOVA with post-hoc Tukey's multiple comparisons test for WT PGM *vs*. AOX PGM+Az; WT PGM *vs*. WT Rot/Succ; AOX PGM *vs*. AOX PGM+Az; AOX PGM *vs*. WT Rot/Succ. PGM, pyruvate, glutamate, malate; Rot, rotenone; Succ, succinate. Note, reliable P/O ratios cannot be determined for mitochondria respiring on succinate in the presence of AOX. (**G**) Respiratory rates of isolated heart mitochondria shown as mean ± SD, n = 3. ADP in µM; Pyr, pyruvate; Glut, glutamate; Mal, malate; n-PG, n-propyl gallate. Grey areas indicate significant difference between WT and AOX ($P < 0.05$) analyzed by 2way ANOVA with post-hoc Sidak's multiple comparisons test. Note, n-PG was added to visualize that respiration in AOX mitochondria was indeed due to catalytic AOX engagement under the conditions described. (**H**) Hydrogen peroxide production shown as mean ± SD, n = 3. Grey areas indicate significant difference between WT and AOX

($P < 0.05$) analyzed by 2way ANOVA with post-hoc Sidak's multiple comparisons test. Note the inverse relation of hydrogen peroxide production and respiratory rate.

Highlights

- Respiratory inhibition poses metabolic stress leading to human pathologies
- Changes of the quinone (Q) pool redox poise reflects metabolic states
- Where expressed, alternative oxidase (AOX) relieves metabolic stress by oxidizing Q
- Ciona AOX was used to study mouse respiratory control mechanisms

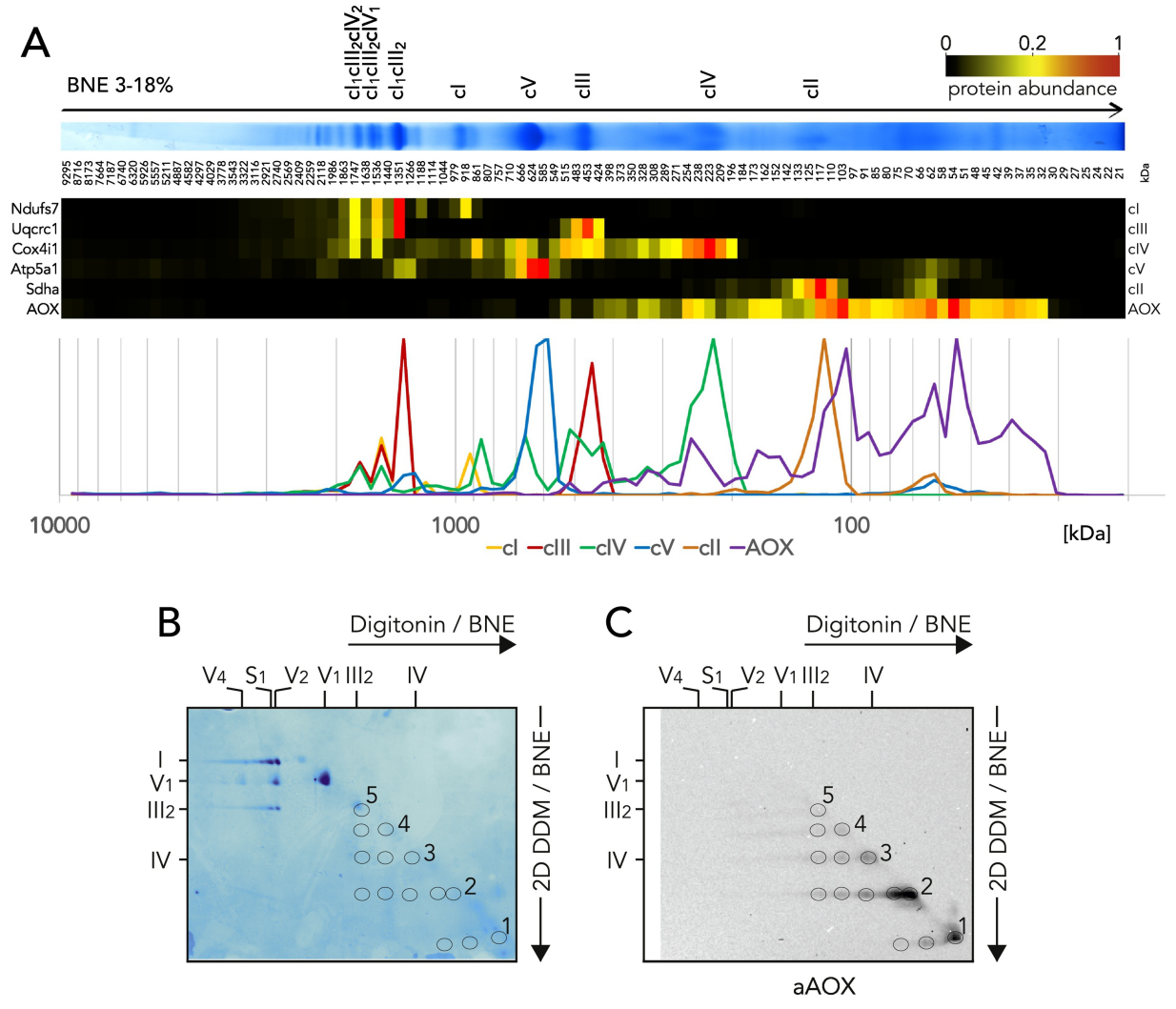
A
BNE 3-18%
cI1cIII2cIV2
cI1cIII2cV1
cI1cIII2
cI
cV
cIII
cIV
cII
0
0,2
1
protein abundance
kDa
Ndufs7
Uqcrc1
Cox4i1
Atp5a1
Sdha
AOX
cI
cIII
cIV
cV
cII
AOX
10000
1000
100
[kDa]
cI cIII cIV cV cII AOX
B
Digitonin / BNE
V4 S1 V2 V1 III2 IV
I
V1
III2
IV
5
4
3
2
1
2D DDM / BNE
C
Digitonin / BNE
V4 S1 V2 V1 III2 IV
I
V1
III2
IV
5
4
3
2
1
2D DDM / BNE
aAOX

Figure 1

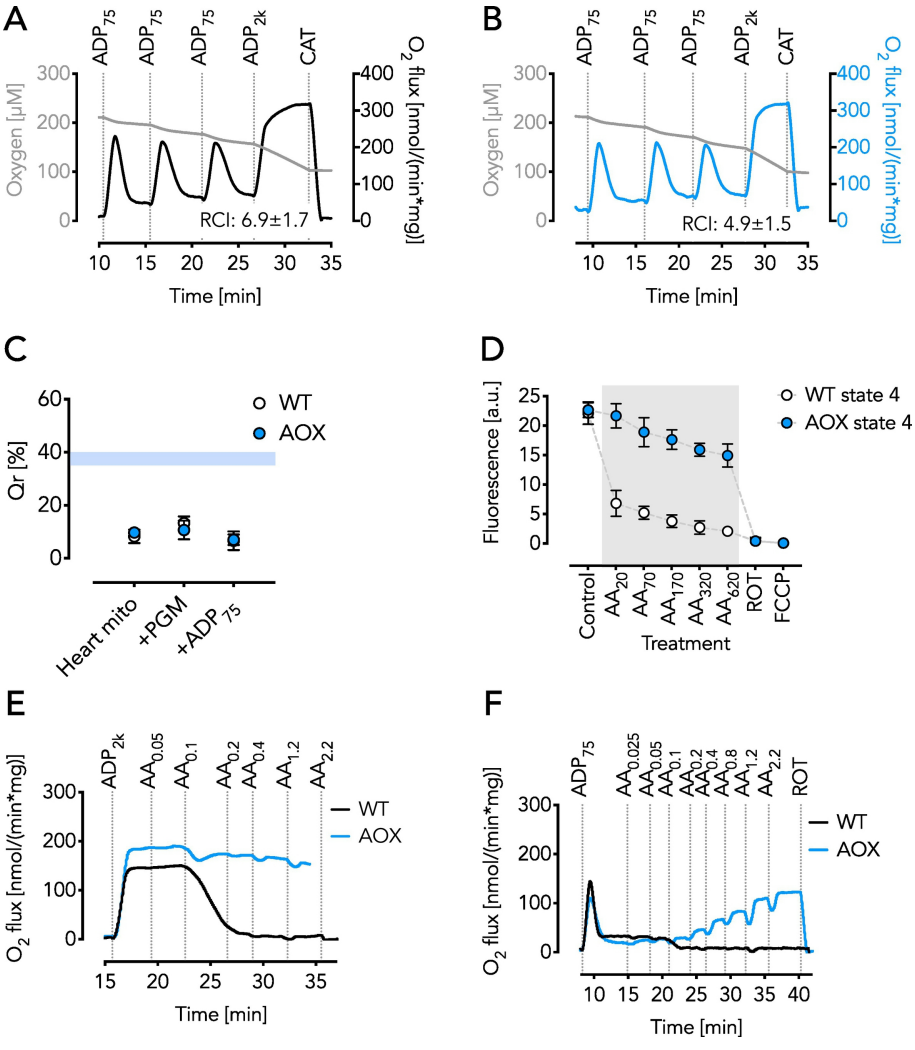
A
B
ADP75
ADP75
ADP75
ADP2k
CAT
Oxygen [µM]
O2 flux [nmol/(min*mg)]
RCI: 6.9±1.7
RCI: 4.9±1.5
Time [min]
C
WT
AOX
Qr [%]
Heart mito
+PGM
+ADP 75
D
WT state 4
AOX state 4
Fluorescence [a.u.]
Control
AA20
AA70
AA170
AA320
AA620
ROT
FCCP
Treatment
E
F
ADP2k
AA0.05
AA0.1
AA0.2
AA0.4
AA1.2
AA2.2
AA0.025
AA0.8
ROT
WT
AOX
O2 flux [nmol/(min*mg)]
Time [min]

Figure 2

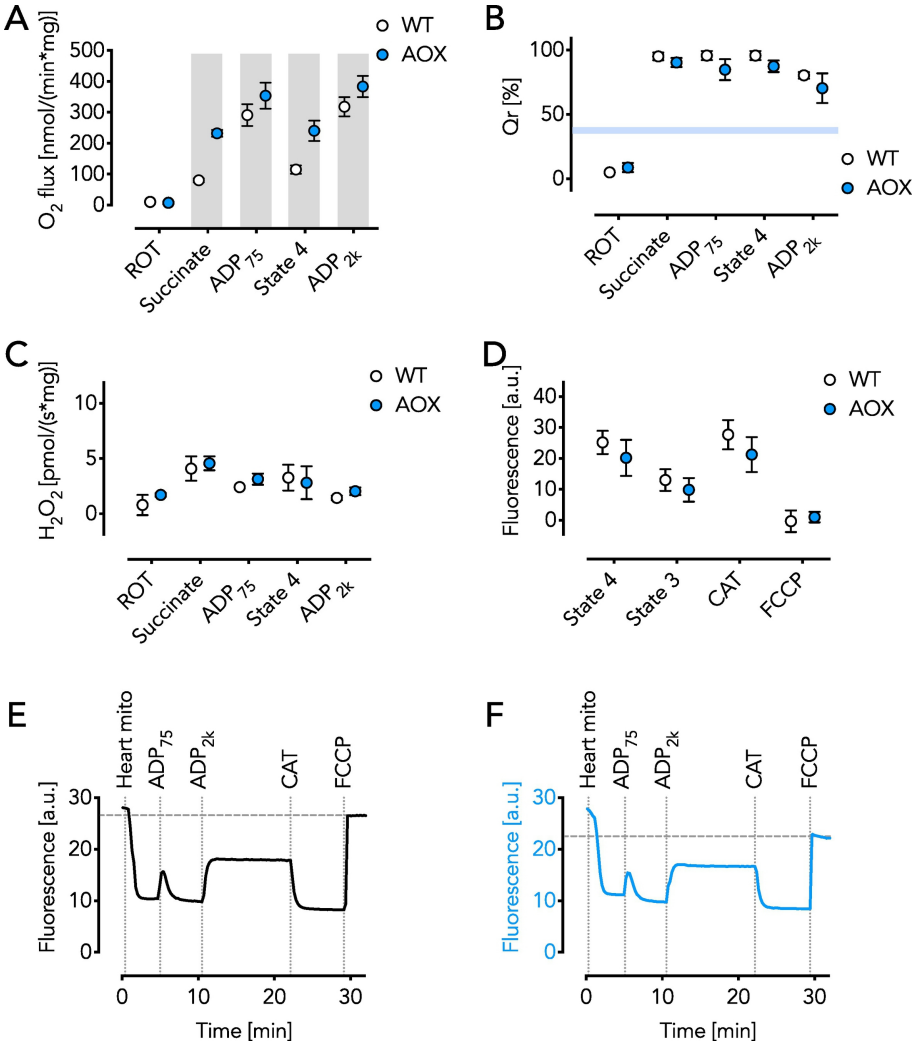
A
O2 flux [nmol/(min*mg)]
500
400
300
200
100
0
WT
AOX
ROT
Succinate
ADP 75
State 4
ADP 2k
B
Qr [%]
100
50
0
WT
AOX
ROT
Succinate
ADP 75
State 4
ADP 2k
C
H2O2 [pmol/(s*mg)]
10
5
0
WT
AOX
ROT
Succinate
ADP 75
State 4
ADP 2k
D
Fluorescence [a.u.]
40
30
20
10
0
WT
AOX
State 4
State 3
CAT
FCCP
E
Fluorescence [a.u.]
Heart mito
ADP75
ADP2k
CAT
FCCP
30
20
10
0
0
10
20
30
Time [min]
F
Fluorescence [a.u.]
Heart mito
ADP75
ADP2k
CAT
FCCP
30
20
10
0
0
10
20
30
Time [min]

Figure 3

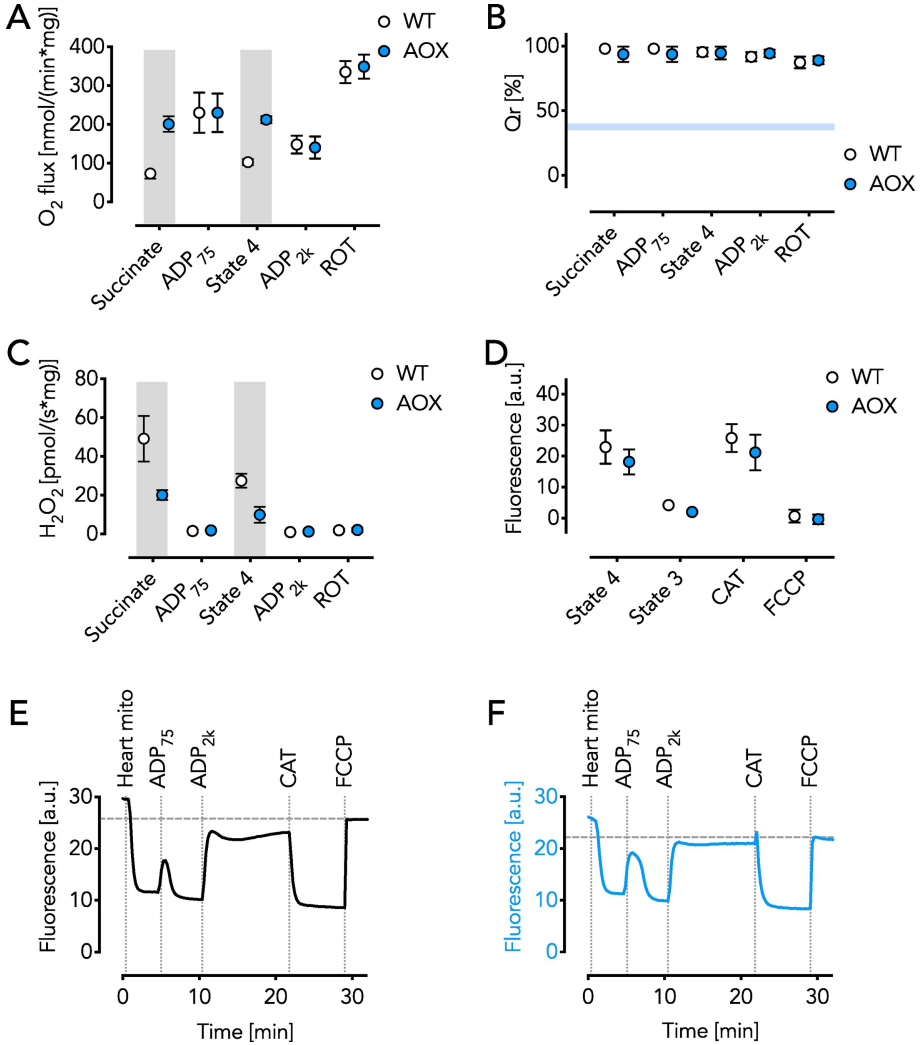
A
O2 flux [nmol/(min*mg)]
400
300
200
100
0
WT
AOX
Succinate
ADP 75
State 4
ADP 2k
ROT
B
Qr [%]
100
50
0
WT
AOX
Succinate
ADP 75
State 4
ADP 2k
ROT
C
H2O2 [pmol/(s*mg)]
80
60
40
20
0
WT
AOX
Succinate
ADP 75
State 4
ADP 2k
ROT
D
Fluorescence [a.u.]
40
30
20
10
0
WT
AOX
State 4
State 3
CAT
FCCP
E
Fluorescence [a.u.]
Heart mito
ADP75
ADP2k
CAT
FCCP
30
20
10
0
0
10
20
30
Time [min]
F
Fluorescence [a.u.]
Heart mito
ADP75
ADP2k
CAT
FCCP
30
20
10
0
0
10
20
30
Time [min]

Figure 4

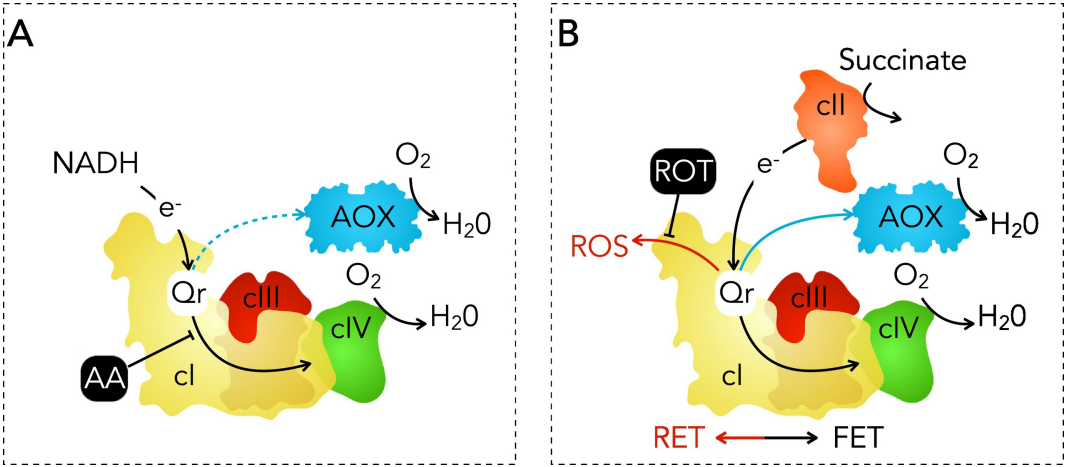
A
NADH
e-
O2
AOX
H20
Qr
cIII
O2
H20
cIV
AA
cI
B
Succinate
cII
ROT
e-
O2
AOX
H20
ROS
Qr
cIII
O2
H20
cIV
cI
RET
FET

Figure 5